The Orientation of Semifluorinated Alkanes Attached to Polymers at the Surface of Polymer Films

Jan Genzer,*,‡,§ Easan Sivaniah,‡ Edward J. Kramer,‡,|| Jianguo Wang,⊥,# Hilmar Körner,⊥,& Maoliang Xiang,⊥ Kookheon Char,⊥,* Christopher K. Ober,⊥ Benjamin M. DeKoven,□ Robert A. Bubeck,△ Manoj K. Chaudhury,☆ Sharadha Sambasivan,◇ and Daniel A. Fischer◇,○

Department of Chemical Engineering, North Carolina State University, Raleigh, North Carolina 27695-7905; Materials Department, University of California at Santa Barbara, Santa Barbara, California 93106-5050; Department of Materials Science & Engineering, Cornell University, Ithaca, New York 14853-1501; Intevac, Santa Clara, California 95054-2704; R. A. B. Consulting, Midland, Michigan 48640; Department of Chemical Engineering, Lehigh University, Bethlehem, Pennsylvania 18015; National Synchrotron Light Source, Brookhaven National Laboratory, Upton, New York 11973; and Material Science & Engineering Laboratory, National Institute for Standards and Technology, Gaithersburg, Maryland 20899

Received July 20, 1999

ABSTRACT: The surface molecular orientation of a liquid crystalline (LC) layer made up of semifluorinated (SF) single side groups [$-CO-(CH_2)_{x-1}-(CF_2)_yF$] (single SF groups) attached to polyisoprene homopolymer or the isoprene block of a styrene−isoprene diblock copolymer was determined by analyzing the partial electron yield C-edge NEXAFS signal. The results show that the surfaces of thin SF polymer films are covered with a uniform layer, consisting of the SF−LC groups whose average $-CF_2-$ tilt angle with the surface normal lies in the range 29−46°. This is in direct contrast to the bulk, where the directors of the SF−LC mesogens are aligned parallel to the polystyrene/SF−polyisoprene interface of the block copolymers. This average tilt angle increases with increasing the length of the $-(CH_2)_{x-1}-$ group (x increases) but decreases with increasing the length of the $-(CF_2)_y-$ part of the molecule (y increases) at constant x.

1. Introduction

To develop polymers with low surface energies, it is common to attach a fluorinated group onto a polymer backbone in order to create a fluorinated surface coating. Commercially available fluorinated ester side group acrylic and methacrylic polymers are typical low surface energy coating materials.[1] Small amounts of fluorinated polymer can also be mixed with or chemically bound to the surface of another polymer to dramatically alter its surface properties.[2] One critical problem, surface reconstruction in contact with polar liquids, still has not been solved, and this limits the practical application of these materials.

A uniformly organized trifluoromethyl ($-CF_3$) array would create a surface with the lowest possible surface tension. Self-assembled monolayers (SAM), produced by self-organization of randomly oriented molecules from a solution or vapor onto a surface, can result in such arrays[3] but are impractical for large-scale applications, especially for coatings on elastomers. An effective approach that avoids SAM techniques for production of uniform $-CF_3$ surfaces is to harness the self-assembly behavior of a class of fluorinated materials, the semifluorinated (SF) alkanes.[4] In addition, to prevent surface reconstruction processes from occurring, it would be ideal also for SF side groups to form liquid crystalline (LC) phases that would effectively "freeze" the surface structure. Bearing this idea in mind, we see that self-organization of SF−LC mesogens on the nanometer length scale could play an important role in the design of stable, low surface energy materials.

Styrene−isoprene diblock copolymers were synthesized, in which semifluorinated [$-CO-(CH_2)_{x-1}-(CF_2)_yF$] side groups were attached to the isoprene block.[5] We refer to such copolymers as SF diblock copolymers (SFDs). Our previous experiments indicated that the morphology of SFDs is governed by the volume ratio of the different blocks (LC or amorphous−lamellar, cylinder) and the structure within the LC block is controlled by the lengths of the side groups. Depending on the x/y ratio, either smectic-A, smectic-B (S_B), or isotropic phases exist. The relationship between the order of the mesogenic SF side groups and the microphase formation has been investigated by small-angle X-ray scattering (SAXS), transmission electron microscopy (TEM), and time-resolved X-ray diffraction.[5] It was found that the SF side groups prefer to pack such that they lie parallel to the styrene/SF−isoprene interface. A detailed analysis of the X-ray data demonstrated that the SF side groups arrange in a liquid crystalline hexagonal S_B phase (similar to precursors). Contact angle measure-

* Corresponding author.
† North Carolina State University.
‡ University of California at Santa Barbara.
§ Present address: Department of Chemical Engineering, North Carolina State University, Raleigh, NC 27695-7905.
|| Also at: Department of Chemical Engineering, University of California at Santa Barbara, Santa Barbara, CA 93106-5080.
⊥ Cornell University.
Present address: Polymer Core Technology, Corning Incorporated, Corning, NY 14831.
& Present address: Institut für Chemie der Kunststoffe, Montanuniversität Leoben, 8700 Leoben, Austria.
○ Permanent address: Department of Chemical Engineering, Seoul National University, Seoul 151-742, Korea.
□ Intevac.
△ Michigan Molecular Institute, Midland, Michigan 48640.
☆ Lehigh University.
◇ Brookhaven National Laboratory
○ National Institute for Standards and Technology.

10.1021/ma991182o CCC: $19.00
Published on Web 02/15/2000

ments revealed a very low surface energy consistent with close packing of $-CF_3$ groups at the surface.[5] These results imply that the SF side groups do not have the same orientation at the surface as they do in the bulk. These SF surfaces proved highly resistant to reconstruction in water, a resistance that might possibly originate in the stabilizing influence of a S_B LC surface ordering of the SF side groups.

It is thus of great interest to probe the near-surface orientation of the LC side groups in SFDs using a truly surface sensitive technique. Near-edge X-ray absorption fine-structure (NEXAFS) has proven to be a powerful tool for studying molecular orientation of a variety of materials.[6] The ability to probe structures at the surface and in the bulk of the material at the same time, along with its high sensitivity to the character and orientation of chemical bonds make NEXAFS superior to other surface methods for this purpose.[7,8] Because sharp core level excitations for C and F occur in the soft X-ray spectral region, NEXAFS is an ideal technique for probing molecular orientations of SFDs.

2. Experiment

2.1. Materials and Sample Preparation. A detailed description of the synthesis of the SF polymers used in this study is given in ref 5. The same block copolymer, which had polystyrene (PS) and polyisoprene (PI) (60% of 1,2 and 40% of 3,4 PI units) blocks, was used as the basic backbone to which the single SF side groups were attached. SF side groups $[-CO-(CH_2)_{x-1}-(CF_2)_yF]$ with various combinations of x and y (BC−FyHx) were attached to the pendent double bonds of the isoprene. Depending on the relative fraction of PS and SF−PI in the copolymer, either spherical, cylindrical, or lamellar bulk morphologies were formed, as detected by both SAXS and TEM. To investigate the role of the copolymer morphology on the organization of the SF groups, the same single SF side groups were also attached to the backbone of PI homopolymer (H−FyHx). In addition, to uncover the role of SF group chemical composition, samples were synthesized in which only the fluorinated part of the side groups was attached to the PI backbone of PS-*b*-PI copolymer (BC−Fy). Differential scanning calorimetry experiments showed that these BC−Fy moieties did not exhibit LC behavior detected in BCFyHx samples. Thin (ca. 50 nm) films of SFDs were prepared by spin-coating solutions of the block copolymers in α,α,α-trifluorotoluene (TFT) onto silicon wafers. The samples were then annealed in a vacuum at 150 °C for 4 h to perfect the bulk and surface morphologies.

2.2. NEXAFS Principles and Instrumentation. NEXAFS involves the resonant X-ray excitation of a K or L shell electron to an unoccupied low-lying antibonding molecular orbital of σ symmetry, σ^*, or π symmetry, π^*.[6] The initial state K shell excitation gives NEXAFS its element specificity, while the final-state unoccupied molecular orbitals provide NEXAFS with its bonding or chemical selectivity. A measurement of the intensity of NEXAFS spectral features enables the identification of chemical bonds and a determination of their relative population density within the sample. Because of the fixed geometry and the fact that the 1s → σ^* and 1s → π^* excitations are governed by dipole selection rules, the resonance intensities vary as a function of the direction of the electric vector **E** of the incident polarized X-ray relative to the symmetry of the molecule.

The NEXAFS experiments were carried out on the NIST/Dow materials characterization end-station at the National Synchrotron Light Source at Brookhaven National Laboratory. The U7A beamline is equipped with toroidal mirror spherical grating monochromator. The incident photon energy resolution and intensity were 0.2 eV and 5×10^{10} photon/s, respectively, for an incident photon energy of 300 eV and a typical storage ring current of 500 mA. The materials characterization end-station is equipped with a heating/cooling stage positioned on a goniometer, which controls the orientation of the sample with respect to the polarization vector of the X-rays. A differentially pumped ultrahigh vacuum compatible proportional counter is used for collecting the fluorescence yield (FY) signal.[9] In addition, the partial-electron-yield (PEY) signal is collected using a channeltron electron multiplier with an adjustable entrance grid bias (EGB). A crude depth profiling within the top 5 nm is possible by increasing the negative EGB on the channeltron detector, at the highest bias thus selecting only the Auger electrons which have suffered negligible energy loss. The monochromator energy resolution and photon energy were calibrated by comparing the transmission spectrum from gas-phase carbon monoxide with electron energy-loss reference data. To eliminate the effect of incident beam intensity fluctuations and monochromator absorption features, the FY and PEY signals were normalized by the incident beam intensity obtained from the photo yield of a clean gold grid.

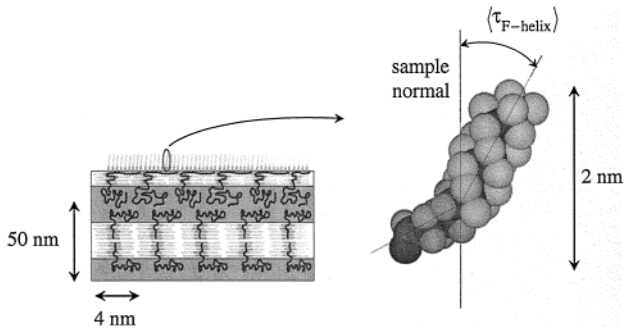

Figure 1. Schematic illustrating the organization of the single SF side groups $[-CO-(CH_2)_{x-1}-(CF_2)_yF]$ in the bulk and on the surface of the SF polymer film made of a symmetric PS/SF−PI diblock copolymer that exhibits lamellar morphology in the bulk.

3. Results

As mentioned in the Introduction, previous SAXS and TEM experiments indicated that, depending on the volume fraction of the PS and the SF−PI blocks in the copolymer, the bulk morphology of the SF polymers consists of either spheres on the bcc lattice, hexagonally organized cylinders, or stacks of alternating lamellae. In addition, it was found that the directors of the SF−LC groups lie always parallel to the PS/SF−PI interfaces. While the organization of the SF−LC groups in the bulk of a thin film depends on the orientation of the copolymer phases that, in turn, is dictated by wetting behavior at the polymer/substrate and polymer/air interfaces, the structure of SF−polymer films at the polymer/air interface is expected to be strongly influenced by the surface tension difference between the PS and the SF−PI blocks and thus may be independent of the bulk sample morphology. Bearing in mind that the $-CF_3$ ends are the lowest surface energy components, we expect the surfaces of the SF films to consist of the SF−PI component. A clear indication of such behavior comes from previous XPS experiments and contact angle measurements.[5] Constructing Zisman plots from the wetting experiments using a homologous series of alkanes also indicated that the critical surface tensions of the surfaces of the SF polymer films are between those expected for those of pure $-CF_3$ and $-CF_2-$ units but close to that of a pure $-CF_3$ surface.[5] On the basis of these measurements the single SF groups on the surfaces of the SF polymer films are expected to only slightly deviate from the sample normal. A schematic of the expected organization of the SF groups in the SF thin films with lamellar bulk morphology is shown in Figure 1. Figure 1 also indicates that the fluorocarbon

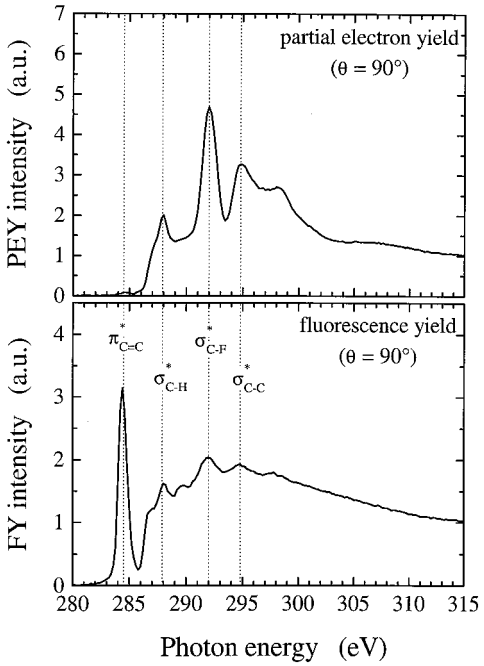

Figure 2. PEY (upper part) and FY (lower part) NEXAFS spectra (solid lines) from the BC−F8H4 sample at EGB = −150 V and $\theta = 90°$. The dotted lines in the figure denote the 1s → σ^* transitions for the C−H (E = 287.9 eV), C−F (E = 292.0 eV), and C−C (E = 294.8 eV) bonds (present in both the PEY and FY NEXAFS spectra) and the 1s → π^* transition of the C═C bond (E = 284.5 eV) in the benzene ring of PS present only in the FY NEXAFS spectrum.

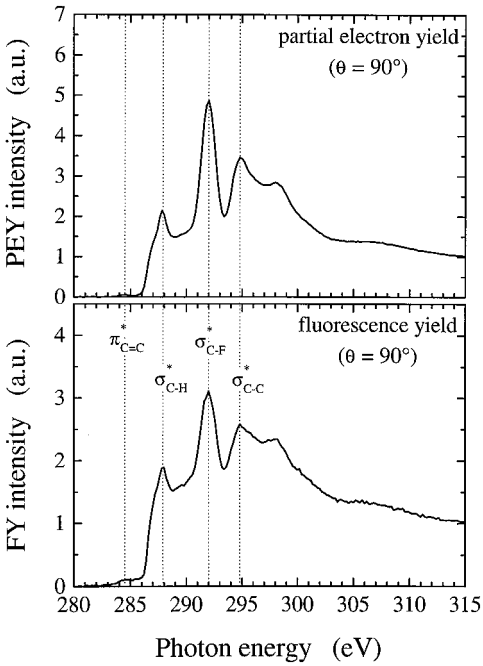

Figure 3. PEY (upper part) and FY (lower part) NEXAFS spectra (solid lines) from the H−F8H4 sample at EGB = −150 V and $\theta = 90°$. The dotted lines in the figure denote the 1s → σ^* transitions for the C−H (E = 287.9 eV), C−F (E = 292.0 eV), and C−C (E = 294.8 eV) bonds.

and the hydrocarbon parts of the single SF groups have in general different average tilt angles with the sample surfaces. In this work we only concentrate on the average tilt angle of the fluorocarbon part of the single SF groups, $\langle\tau_{F-helix}\rangle$.

Because the length of the single SF groups (ca. 2 nm) is comparable with the escape depth of Auger electrons that are produced during the NEXAFS experiments, detecting the partial electron yield (PEY) NEXAFS signal will help us to analyze the orientation of the single SF groups on the sample surfaces. Moreover, by simultaneously detecting the fluorescence yield (FY) NEXAFS signal, which originates from the entire sample, we can also gain insight into the organization of the whole sample. Figure 2 shows the PEY (upper part) and FY (lower part) NEXAFS signals from the BC−F8H4 sample positioned perpendicular to the X-ray beam ($\theta = 90°$). From inspection of Figure 2, several characteristic peaks are seen to be present in both the PEY and FY NEXAFS spectra. These correspond to the 1s → σ^* transitions associated with the C−H (E = 287.9 eV), C−F (E = 292.0 eV), and C−C (E = 294.8 eV) bonds. Moreover, the FY spectrum exhibits one more strong signal at E = 284.5 eV, which is missing in the PEY spectrum. This peak can be associated with the 1s → π^* transition of the C═C bond in the phenyl ring of PS. Comparing the PEY and FY NEXAFS spectra thus reveals two pieces of information. First, there is no PS present on the surface of the sample; second, the PEY NEXAFS signal can be exclusively used to probe the organization of the single SF groups at surfaces of the SF thin films. To reinforce this point, in Figure 3 we show the PEY and FY NEXAFS spectra taken from the H−F8H4 sample with the same geometry as the BC−F8H4 sample. As mentioned earlier, no PS is present

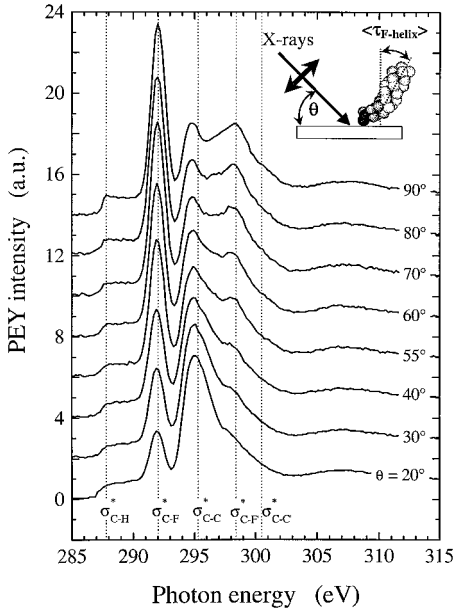

Figure 4. PEY NEXAFS spectra of SF−SAM (SiO_x) sample at EGB = −150 V and various sample orientations with respect to the X-ray beam, θ. The inset shows schematically the sample geometry.

in this sample. Figure 4 shows that while the C−H, C−F, and C−C 1s → σ^* transitions can still be observed, no peak that would correspond to the 1s → π^* transition in the phenyl ring of PS is seen. Figures 2 and 3 thus demonstrate the strength of NEXAFS in simultaneously probing both the surface and the bulk structures of thin films.

To resolve the molecular orientation on the SF polymer film surfaces, NEXAFS experiments were first carried out on a sample consisting of a well-ordered self-assembled semifluorinated monolayer whose structure $[-O_{1.5}Si-(CH_2)_2-(CF_2)_8F]$ closely resembles that of the

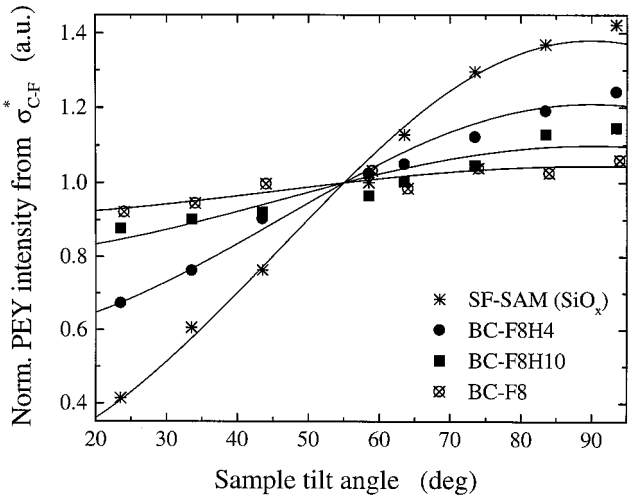

Figure 5. Normalized PEY NEXAFS intensities vs sample tilt angle from σ^* C−F bond in C 1s for SF−SAM (SiO_x) (stars), BC−F8H4 (closed circles), BC−F8H10 (closed squares), and BC−F8 (crossed circles). The solid lines were obtained by fitting the experimental data using the "modified building block" model method described in ref 12.

SF−LC side groups in SF polymers.[4] We further refer to this sample as SF−SAM (SiO_x). These experiments provided important benchmarks for interpreting the NEXAFS results on the SF polymers. Figure 4 shows the PEY NEXAFS spectra at the C 1s edge from SF−SAM (SiO_x) sample measured at entrance grid bias (EGB) of the channeltron electron multiplier of −150 V and eight different angles θ between the sample normal and the polarization vector of the X-ray beam. The dotted lines denote the positions of the 1s → σ^* transitions for the C−H, C−F, and C−C bonds. The fact that the intensities originating from these transitions change with varying angle θ (as θ increases the intensity corresponding to the 1s → σ^* transitions of the C−F bond increases while that of the C−C bond decreases) indicates that the SF molecules are well oriented.

Similar experiments were carried out on the SF polymer films with various combinations of x and y. In particular, two series of SF polymers were studied in which either x was kept constant and y was varied or vice versa. Following the method proposed by Outka and co-workers,[10] the PEY NEXAFS spectra were fitted to a series of Gaussian curves and a step function corresponding to the excitation edge of carbon. The corresponding intensities of the C−F signal at different θ values from selected SF samples investigated in this project are presented in Figure 5. Figure 5 shows the normalized PEY σ^* C−F bond NEXAFS intensities vs θ for SF−LC groups in BC−F8H4 (closed circles) and BC−F8H10 (closed squares). Included in Figure 5 are also the data for SF−SAM (SiO_x) (crosses) and BC−F8 (crossed circles). The latter two data sets represent benchmark samples that exhibit the highest orientation and no orientation, respectively. The actual PEY NEXAFS intensities in Figure 5 have been normalized with respect to the intensity at the "magic angle", $\theta = 54.7°$.[11] Clearly, the fact that the intensity of the σ^* C−F signal changes when the sample tilt angle is varied indicates that the SF−LC groups at the surface of the SF polymer films are oriented. Bearing in mind that the steeper the slope of the intensity vs sample tilt angle, the smaller is the deviation of the molecular main axis from the substrate normal, the results in Figure 5 illustrate that

Table 1. Average Tilt Angle, $\langle\tau_{F-helix}\rangle$, of the Fluorocarbon Chains in the SFDs

sample	x	y	$\langle\tau_{F-helix}\rangle$ (deg)	note
SF−SAM (SiO_x)	2	8	4 ± 2	*a*
BC−FB8		8	51 ± 5	*b*
BC−F8H4	4	8	33 ± 3	*c*
H−F8H4	4	8	29 ± 3	*d*
BC−F8H6	6	8	35 ± 2	*c*
BC−F8H10	10	8	43 ± 3	*c*
H−F8H10	10	8	44 ± 4	*d*
FB−F6H10	10	6	46 ± 1	*c*
FB−F10H10	10	10	38 ± 3	*c*

[a] SF−SAM (SiO_x): self-assembled monolayer made of $-O_{1.5}Si-(CH_2)_2-(CF_2)_8F$ attached to the surface of silicon oxide. [b] BC−Fy: PS-*b*-PI copolymer with a single $-CO-(CF_2)_yF$ group attached to the PI block. [c] BC−FyHx: PS-*b*-PI copolymer with a single $-CO-(CH_2)_{x-1}-(CF_2)_yF$ group attached to the PI block. [d] H−FyHx: PI homopolymer with a single $-CO-(CH_2)_{x-1}-(CF_2)_yF$ group.

$\langle\tau_{F-helix}\rangle$ for the BC−F8Hx copolymers is larger than $\langle\tau_{F-helix}\rangle$ for the SF−SAM (SiO_x) sample but smaller than $\langle\tau_{F-helix}\rangle$ of the non-LC BC−F8 polymer. Moreover, in samples where y is held constant ($y = 8$), $\langle\tau_{F-helix}\rangle$ on the surface relative to the sample normal increases with increasing x. Systematic measurements of surface orientation have been carried out on two series of SF polymer films, in which (a) $y = 8$ and x was varied, and (b) $x = 10$ and y was varied.

To quantify the measured PEY NEXAFS intensities vs sample tilt, a model was developed in the spirit of the "modified building block" approach. The details of the model are described elsewhere;[12] here we restrict ourselves to only a brief summary. In the model we assumed that the $-CH_2-$ spacer adopts a planar zigzag structure, e.g., polyethylene, and the $-CF_2-$ part has a helical structure 15/7, e.g., poly(tetrafluoroethylene). The original building block model proposed by Stöhr and co-workers[5,10] was modified such that the NEXAFS intensity originating from a σ^* orbital was corrected for the energy loss of the Auger electrons originating from the subsurface regions of the sample. By analyzing several data sets collected from the same sample and different entrance grid biases of the channeltron electron multiplier, we were able to determine $\langle\tau_{F-helix}\rangle$.

The results of the fits using the modified building block model on the experimental data taken from the BC−F8Hx/H−F8Hx and BC−FyH10/H−FyH10 series are summarized in Table 1 and plotted in Figure 6. Figure 6a shows the dependence of $\langle\tau_{F-helix}\rangle$ on the number of the $-CH_2-$ units in the SF side groups for BC−F8Hx (closed circles) and H−F8Hx (open circles). The observation that the results for BC−F8H4 samples are close to those for H−F8H4 shows that the constraints of the lamellar block copolymer structure have only a minor effect on the SF side group orientation. The results in Figure 6a demonstrate that keeping the length of the rigid fluorocarbon part of the single SF side group fixed and increasing the length of the hydrocarbon spacer results in a larger $\langle\tau_{F-helix}\rangle$. Figure 6b displays the dependence of $\langle\tau_{F-helix}\rangle$ on the number of the $-CF_2-$ units in the SF side groups for BC−FyH10 (closed circles) and H−FyH10 (open circles). As for the BC−F8H4/H−F8H4 samples, the average tilt angles of the fluorocarbon part of the SF chain in BC−F8H10/H−F8H10 couples are very similar. Moreover, the results in Figure 6b show that at constant x, $\langle\tau_{F-helix}\rangle$ decreases modestly with increasing y. The results

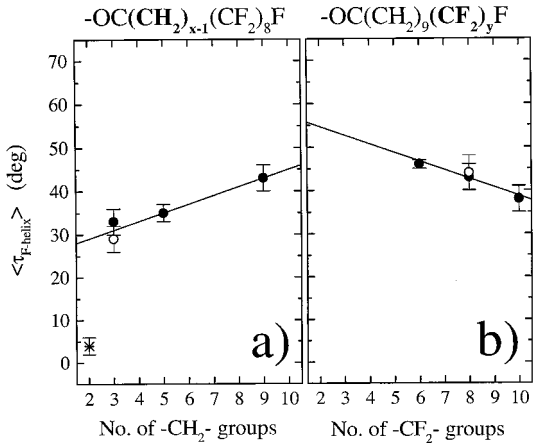

Figure 6. Average tilt angles of the fluorocarbon helix, $\langle\tau_{F-helix}\rangle$, vs the number of the a) $-CH_2-$ units and (b) $-CF_2-$ units in the single SF side group. The closed and open circles correspond to the BC−F*y*H*x* and H−F*y*H*x* samples, respectively, and the cross denotes $\langle\tau_{F-helix}\rangle$ measured on the surfaces of the SF−SAM (SiO_x) sample. The solid lines are guides to the eye.

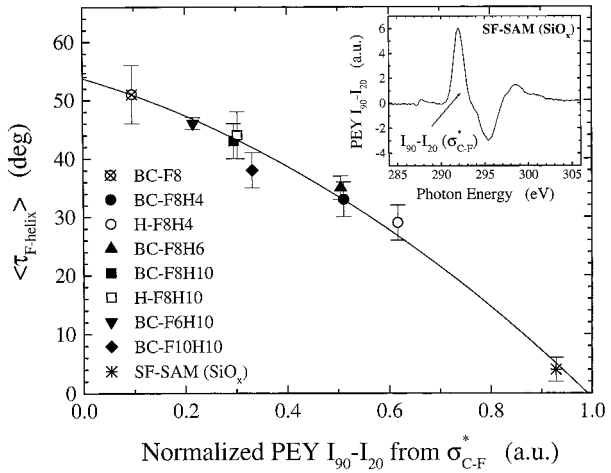

Figure 7. Average tilt angles of the fluorocarbon helix, $\langle\tau_{F-helix}\rangle$, vs the difference in the normalized PEY NEXAFS intensities at $\theta = 90°$ and $\theta = 20°$ at the 1s → σ^* transition for the C−F bond. The solid line is a guide to the eye. The inset shows the difference PEY NEXAFS spectrum from SF−SAM (SiO_x) obtained by subtracting the PEY NEXAFS signal from SF−SAM (SiO_x) measured at $\theta = 20°$ from that at $\theta = 90°$. The filled area represents the difference in the PEY NEXAFS intensities corresponding to the 1s → σ^* transition for the C−F bond.

presented in Figure 6 thus clearly show that an increase in the length of the fluorocarbon part of the single SF group leads to a smaller $\langle\tau_{F-helix}\rangle$. Similarly, decreasing the length of the hydrocarbon spacer leads to smaller $\langle\tau_{F-helix}\rangle$. We note that the above conclusions are valid only for the LC-type SF groups, thus for samples with $x > 1$.

4. Discussion

On the basis of the results of the PEY NEXAFS analysis presented in the previous section several important observations can be made. First, the surfaces of the SF thin polymer films made of PI-containing polymers that are modified by attaching the SF−LC single side groups exhibit an exceptional degree of ordering. It is important to reemphasize that such high surface organization of the single SF groups has been achieved by simply casting the polymers in thin films and annealing them at temperatures above the T_g of the polymers. Second, the combination of the SAXS data and the present NEXAFS analysis reveals that while in the bulk of the BC−F*y*H*x* samples the single SF groups lie parallel to the PS/SF−PI phase boundary, the surfaces of thin SF polymer films are covered with a uniform layer consisting of an array of the SF−LC groups that are on average only slightly tilted from the sample normal. Third, the average tilt of the fluorocarbon part of the single SF groups is determined by the combination of *x* and *y* and is thus exclusively dictated by the molecular structure of the SF groups. As demonstrated in Figure 6 the surface orientation of the single SF groups with the same combination of *x* and *y* on the surface of both diblock copolymer and homopolymer film surfaces is the same. Fourth, independent experiments on diblock copolymer samples with the same SF side groups but with various thicknesses that cause the formation of islands or holes does not disturb the overall measured $\langle\tau_{F-helix}\rangle$.[13] Moreover, as discussed in ref 13, casting the films from different solvents leads to various bulk morphologies but it does not influence $\langle\tau_{F-helix}\rangle$. Overall, the results from the PEY NEXAFS analysis reveal that the average tilt of the SF−LC group is dictated by both the length of the rigid $-CF_2-$ helix and the length of the hydrocarbon units.

Finally, the results on the orientation of the SF−LC group on the surfaces of the various SF polymer films presented in this work can be used to construct a master curve that allows one to determine $\langle\tau_{F-helix}\rangle$ from only two PEY measurements at $\theta = 90$ and $\theta = 20°$. Figure 7 shows $\langle\tau_{F-helix}\rangle$ as a function of the difference in the normalized PEY NEXAFS intensities at $\theta = 90°$ and $\theta = 20°$ for all single SF groups samples studied (the various symbols corresponds to the various samples under investigation). Figure 7 demonstrates that regardless of the nature of the polymer (copolymer vs homopolymer), $\langle\tau_{F-helix}\rangle$ follows the general trend: namely, $\langle\tau_{F-helix}\rangle$ increases with increasing *x* and/or decreasing *y*. The master curve in Figure 7 can be used to predict the average tilt values of the fluorocarbon part of the single SF chains just by measuring the PEY NEXAFS intensities at $\theta = 90°$ and $\theta = 20°$.

5. Conclusion

NEXAFS is used to study the molecular ordering on surfaces of polystyrene/SF−polyisoprene diblock copolymer and SP−polyisoprene films in which the polyisoprene block is modified by attaching semifluorinated $[-CO-(CH_2)_{x-1}-(CF_2)_yF]$ side groups that exhibit liquid crystalline order. The PEY NEXAFS signal reveals that, in contrast to the bulk, where the directors of the SF−LC mesogens prefer to align parallel to the polystyrene/SF−polyisoprene interface of the block copolymers, the SF−LC groups on the surfaces of SFDs are on average only slightly tilted from the sample normal. In samples where perfluoroalkane length, *y*, is held constant, this average tilt, $\langle\tau_{F-helix}\rangle$, increases with increasing hydrocarbon length, *x*. Similarly, in samples with constant *x*, increasing *y* leads to smaller $\langle\tau_{F-helix}\rangle$ and more erect perfluoroalkane groups.

Acknowledgment. This research was supported by the Office of Naval Research, Grant No. N00014-92-J-1246. Partial support from Division of Materials Research, NSF Polymer Program, Grants No. DMR92-23099 and DMR93-214573, is also appreciated. The

work at NC State University was supported by the NCSU COE start-up funds and the NSF CAREER award, Grant No. DMR98-75256. The authors thank Dr. B. Glüsen and Ms. S. Yang (Cornell University) for their assistance during the course of the NEXAFS experiments. K.C. greatly acknowledges the financial support from the LG-Yonam Foundation for a sabbatical visit to Cornell University (1997−1998). NEXAFS experiments were carried out at the National Synchrotron Light Source, Brookhaven National Laboratory, which is supported by the U.S. Department of Energy, Division of Materials Sciences and Division of Chemical Sciences. This work made use of MRL Central Facilities at UCSB supported by the National Science Foundation under Grant No. DMR96-32716.

References and Notes

(1) Pittman, A. G. In *Fluoropolymers*; Wall, L. A., Ed.; Wiley: New York, 1972; Vol. 25, p 419. Schmidt, D. L.; Coburn, C. E.; DeKoven, B. M.; Potter, G. E.; Meyers, G. F.; Fisher, D. A. *Nature* **1994**, *368*, 39.

(2) Hwang, S. S.; Ober, C. K.; Perutz, S.; Iyengar, D.; Schneggenburger, L. A.; Kramer, E. J. *Polymer* **1995**, *36*, 1321. Iyengar, D. R.; Perutz, S. M.; Dai, C.-A.; Ober, C. K.; Kramer, E. J. *Macromolecules* **1996**, *29*, 1229.

(3) Ulman, A. *An Introduction to Ultrathin Organic Films—From Langmuir−Blodgett to Self-Assembly*; Academic Press: New York, 1991. Swalen, J. D.; Allara, D. L.; Andrade, J. D.; Chandros, E. A.; Garoff, S.; Israelachvili, J.; McCarthy, T. J.; Murray, R.; Pease, R. F.; Rabolt, J. F.; Wynne, K. J.; Yu, H. *Langmuir* **1987**, *3*, 932. Bain, C. D.; Whitesides, G. M. *Angew. Chem.* **1989**, *101*, 522. Whitesides, G. M.; Labinis, P. E. *Langmuir* **1990**, *6*, 87.

(4) Chaudhury, M. K.; Whitesides, G. M. *Langmuir* **1991**, *7*, 1013.

(5) Wang, J.; Mao, G.; Ober, C. K.; Kramer, E. J. *Macromolecules* **1997**, *30*, 1906.

(6) Stöhr, J. *NEXAFS Spectroscopy*; Springer-Verlag: Berlin, 1992.

(7) Genzer, J.; Sivaniah, E.; Kramer, E. J.; Wang, J.; Körner, H.; Xiang, M.; Yang, S.; Ober, C. K.; Char, K.; Chaudhury, M. K.; DeKoven, B. M.; Bubeck, R. A.; Fischer, D. A.; Sambasivan, S. In *Applications of Synchrotron Radiation Techniques to Materials Science IV*; Mini, S. M., Perry, D. L., Stock, S. R., Terminello, L. J., Eds.; Materials Research Society Symposium Proceedings, Vol. 524; Materials Research Society: Pittsburgh, PA, 1998; p 365.

(8) Fischer, D. A.; Mitchell, G. E.; Yeh, A. T.; Gland, J. L. *Appl. Surf. Sci.* **1998**, *133*, 58.

(9) Fischer, D. A.; Colbert, J.; Gland, J. L. *Rev. Sci. Instrum.* **1989**, *60*, 1596.

(10) Outka, D.; Stöhr, J.; Rabe, J.; Swalen, J. D. *J. Chem. Phys.* **1988**, *88*, 4076.

(11) Due to the nature of the polarization dependencies of the NEXAFS signal intensities, one cannot distinguish between a completely disoriented sample and a sample whose chains are all tilted by 54.7°, the so-called, “magic angle”.

(12) Genzer, J.; Fischer, D. A.; DeKoven, B. M.; Sivaniah, E.; Kramer, E. J.; Char, K.; Ober, C. K.; Bubeck, R. A. To be published.

(13) Genzer, J.; Sivaniah, E.; Kramer, E. J.; Wang, J.; Xiang, M.; Char, K.; Ober, C. K.; Bubeck, R. A.; Sambasivan, S.; Fischer, D. A.; Graupe, M.; Colorado, R., Jr.; Shmakova, O. E.; Lee, T. R. To be published.

MA991182O